Membrane Structure and Permeation Properties of Poly(vinyl Chloride)/Liquid Crystal Composite Membrane

TISATO KAJIYAMA, SHINTARO WASHIZU, and MOTOWO TAKAYANAGI, *Department of Applied Chemistry, Faculty of Engineering, Kyushu University 36, Hakozaki, Higashi-ku, Fukuoka 812, Japan*

Synopsis

A series of polymer/liquid crystal composite membranes, at several weight ratios, was prepared casting from a tetrahydrofuran solution of poly(vinyl chloride) (PVC) with *N*-(4-ethoxybenzylidene)-4'-butylaniline (EBBA). From the thermal analysis, microscopic observation, mechanical property, and gas permeation studies, the properties for a series of PVC/EBBA composite membranes were derived. DSC showed that PVC and EBBA were quite miscible and EBBA in composite membranes at below 30 wt % was molecularly dispersed without forming crystal domains. Morphological observations exhibited that EBBA molecules interpenetrated in a continuous phase among the 3-dimensional spongy networks of PVC matrix in the case of the 40/60 (PVC/EBBA, in wt %) composite membrane. Stable retention of EBBA in the composite membrane and its high mechanical durability might arise from such an aggregation structure. The permeability coefficients to oxygen gas, P_{O_2} and nitrogen one, P_{N_2} through the 40/60 (PVC/EBBA) composite membrane showed a discontinuous jump with a several–tenfold increase in the vicinity of the crystal–nematic transition temperature T_{KN} of EBBA. The magnitudes of P_{O_2} and the separation factors P_{O_2}/P_{N_2} above T_{KN} were of the order of 10^{-9} cm^3 (STP) cm^{-1} s^{-1} cm Hg^{-1} and 2–3, respectively. The value of P_{O_2}/P_{N_2} reached a maximum just above T_{KN}. The $P_{O_2} - P_{O_2}/P_{N_2}$ relationship above T_{KN} exhibited an unusual behavior as P_{O_2}/P_{N_2} increased with an increase in P_{O_2}.

INTRODUCTION

In general, the permeation process of low molecular substances through a homogeneous or nonporous polymeric membrane can be explained by a solution–diffusion mechanism. In the case that a membrane has both characteristics of excellent solubility and diffusivity to specific permeant molecules, the membrane is regarded as a permselective. The solution process depends on the affinity of the membrane for the permeant molecule, as a controlling factor to improve permselectivity. The diffusion process is influenced by the thermal molecular motion of polymeric chains, in other words, the magnitude of free volume or the size of the penetrant molecules.[1] Therefore, the molecular design of a permselective membrane is based on two factors, the solubility and the diffusivity.

Silicone rubber shows the best gas permeability among synthetic polymeric membranes, because of its relatively "loose" structure and prominent thermal molecular motion in the rubbery state. However, since silicone rubber is limited in mechanical toughness and selectivity, various modifi-

Journal of Applied Polymer Science, Vol. 29, 3955–3964 (1984)
 CCC 0021-8995/84/123955-10$04.00

cations, such as copolymerization with polycarbonate or poly(4-methyl-pentene-1) are required for the practical use.[2,3]

Polymer/liquid crystal composite membrane can control solubility and diffusivity on gas permeation by means of the chemical structure and/or excellent fluidity of liquid crystalline materials.[4,5] For a composite membrane composed of mechanically tough matrix polymer, an ultrathin and fairly wide-area membrane is expected, in spite of the fact that the characteristics of this system are analogous to a liquid membrane.

In this article, we have investigated the characteristic membrane structures and permeation properties of poly(vinyl chloride)/liquid crystal composite membrane, on the basis of DSC, stress–strain, and gas permeation studies and, also, polarizing optical and scanning electron microscopic observations.

EXPERIMENTAL

Figure 1 shows the chemical structures of poly(vinyl chloride) (PVC) as a matrix polymer and *N*-(4-ethoxybenzylidene)-4′-butylaniline (EBBA) as a liquid crystalline material for the composite membrane. PVC was obtained from Mitsubishi Monsant Kasei Co., Ltd. (Vinica 37L, $\bar{M}_n$ = 66,000). The crystal–nematic and nematic–isotropic transition temperatures of EBBA are 304 K (T_{KN}) and 355 K (T_{NI}), respectively. PVC/EBBA composite membranes were prepared casting from a tetrahydrofuran solution of PVC with EBBA at 293 K ($< T_{KN}$), at which EBBA was several weight fractions. Ageing was performed at 333 K well above T_{KN} for 2 h in an atmosphere of nitrogen. The weight percentages of PVC/EBBA composite membranes were 100/0, 85/15, 70/30, 55/45, 40/60, and 30/70. Polycarbonate (PC)/EBBA composite membranes were also prepared in a similar manner[4] in order to compare with the permeation properties of PVC/EBBA ones.

Thermal analyses were carried out with DSC (UNIX, Rigaku Denki Co., Ltd.) from 220 to 370 K in an atmosphere of nitrogen. The heating or cooling rate was 10 K · min^{-1} and the sample weight about 25 mg. Instrumental calibration was carried out using Ga and palmitic acid as standard materials.

Membrane surface and fracture one of composite membranes coated with gold were observed using a Hitachi Scanning Electron Microscope (S-430). In order to observe the aggregation states of each component, EBBA in composite membranes was extracted with ethanol at 333 K for 2 h.

The process of membrane formation during a solvent evaporation was investigated with a polarizing optical microscope under crossed nicols at 293 K ($< T_{KN}$).

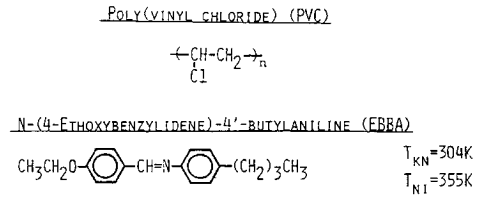

Fig. 1. Chemical structures of PVC and EBBA. T_{KN} and T_{NI} represent crystal–nematic and nematic–isotropic transition temperatures of EBBA, respectively.

Uniaxial stress–strain experiments were made with a tensile tester (Tensilon UTM III-500, Toyo Baldwin Co., Ltd.) at 293 K at the crosshead speed of 20 mm min^{-1}. Samples were die-cut from a sheet of composite membranes of 0.2 mm in thickness. The specimen dimensions were 20 mm in gage length and 5 mm in width.

Oxygen and nitrogen permeations were studied mainly for the 40/60 (PVC/EBBA) composite membrane. The Barrer-type apparatus[6] was used for a permeation experiment. A controlled pressure of the feed side (high-pressure side) was 40–45 cm Hg. An increase in pressure in the permeant side (low-pressure side) was measured with a McLeod gage as a function of time. From the time dependence of amount of permeation, the permeability coefficient P was calculated as usual.

RESULTS AND DISCUSSION

Thermal Properties

In order to elucidate an aggregation or dispersing state of EBBA molecules in a composite membrane, thermal analyses are very useful. Figure 2 shows the differential scanning calorimetric (DSC) curves for PVC, EBBA, and PVC/EBBA composite membranes. Two endothermic peaks were observed for EBBA, which correspond to the crystal–nematic (T_{KN} = 304 K) and nematic–isotropic (T_{NI} = 355 K) transition temperatures, respectively (curve 1 in Fig. 2). These transition processes were also observed at approximately similar temperature ranges for PVC/EBBA composite membranes at which the EBBA fraction was 45–70 wt % [curve 2 for the 40/60 (PVC/EBBA) composite membrane]. However, the PVC/EBBA composite membranes at below the EBBA fraction of 30 wt % did not exhibit such transition peaks on the DSC curve, but this curve deviated from a flat base line at about 300 K (curve 3). This thermal behavior indicates that EBBA

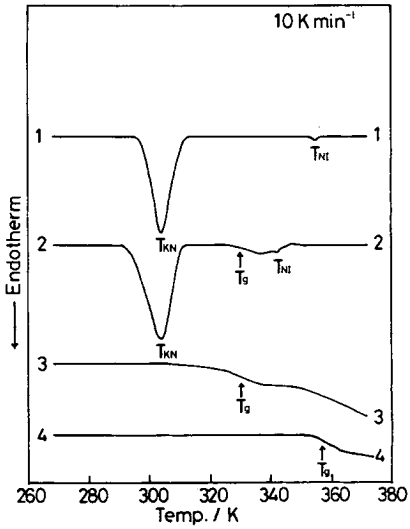

Fig. 2. DSC curves of PVC (4), EBBA (1), and PVC/EBBA [(2) 40/60; (3) 70/30] composite membranes. T_g represents glass transition temperature of PVC.

is molecularly dispersed at below 30 wt %. Therefore, in the case of the EBBA fraction at above 45 wt %, it is clear that EBBA exists in both states of molecular dispersion and crystal domains. The glass transition temperature T_g for PVC homopolymer was observed at about 360 K (curve 4), and it was depressed to about 330 K for composite membranes (curves 2 and 3). The lowering of T_g indicates that PVC and EBBA are quite miscible, and EBBA in composite membranes acts as a plasticizer for PVC.

Microscopic Observation

Figure 3 shows the scanning electron microscopic (SEM) photographs of the fracture surface (upper portion in each photograph) and membrane one (lower portion) for the 40/60 (PVC/EBBA) composite membrane quenched

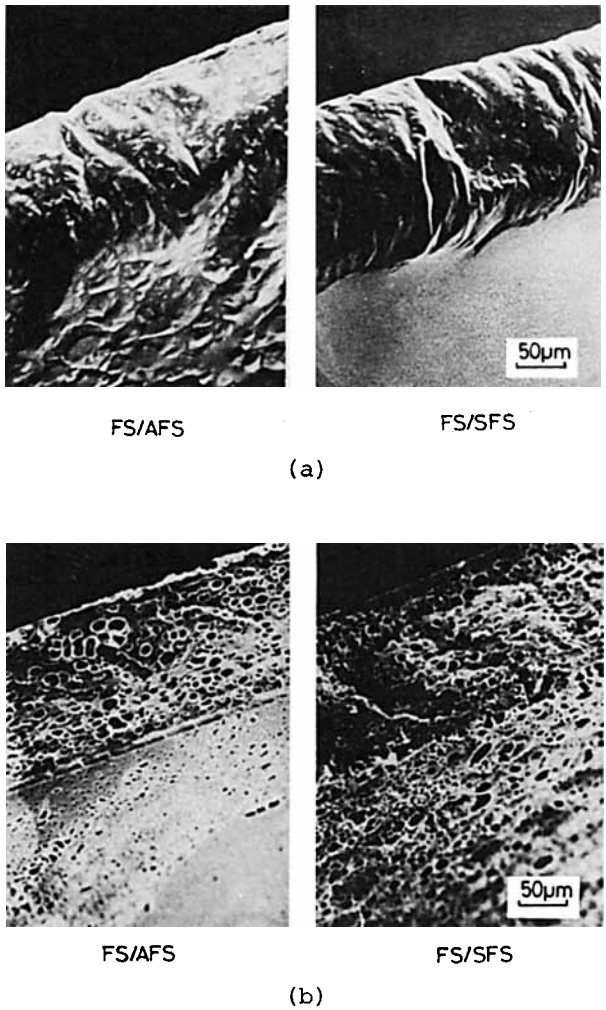

Fig. 3. Scanning electron micrographs of fracture surface (FS) (upper portion in each photograph) and membrane surface (lower portion) for 40/60 (PVC/EBBA) composite membrane. AFS and SFS represent air facing surface and substrate facing surface, respectively: (a) a sample quenched with liq N_2 after annealing at 333 K; (b) a sample after extracting EBBA from (a) with ethanol at 333 K for 2 h.

with liq N_2 after annealing at 333 K ($> T_{KN}$). Annealing was performed in order to observe the surface states of the composite membrane above T_{KN}, since the gas permeation property is remarkably affected by the surface states of membrane, especially above T_{KN}.[7] AFS and SFS represent the air-facing surface and the substrate-facing one when the membrane was cast, respectively. It is apparently observed in Figure 3(a) that EBBA domains are oozing from the membrane surface and spreading over the whole. This oozing tendency of EBBA was more remarkable than the case of the 40/60 (PC/EBBA) composite membrane.[7] The sample after extracting EBBA with ethanol at 333 K for 2 h presents an appearance of spongy material as shown in Figure 3(b). Since about 95 wt % of total EBBA was extracted from the composite membrane with hot ethanol, it is evident that EBBA molecules form domains as an interpenetrating continuous phase among the 3-dimensional spongy networks of PVC matrix. Consequently, it seems reasonable to consider that the continuous EBBA phase takes a role of main diffusing region for gas permeation. In addition, the concentration of EBBA on SFS was relatively a little higher than that on AFS. Thus, the gas permeation experiments in this study were consistently performed by use of the AFS side as a gas feed surface.

Figure 4 shows the SEM photographs for PVC homopolymer (100/0) (a) and the 30/70 (PVC/EBBA) composite membrane (b) after extracting EBBA with hot ethanol. PVC homopolymer did not exhibit any apparent changes even after extraction. On the other hand, the 30/70 (PVC/EBBA) composite membrane presented a noticeable feature, that is to say, the domain size of extracted EBBA further increased than that for the 40/60 (PVC/EBBA) composite membrane and its mean diameter was about 13 μm. This result suggests that the membrane structure of which the spongelike porous membrane is closely filled up with the liquid crystalline material can be prepared by a simple procedure such as casting from a solution of polymer with liquid crystalline materials (up to 70 wt % of EBBA) below T_{KN}.

Furthermore, the formation process of a composite membrane was traced with a polarizing optical microscope (POM). Figure 5 shows the POM pho-

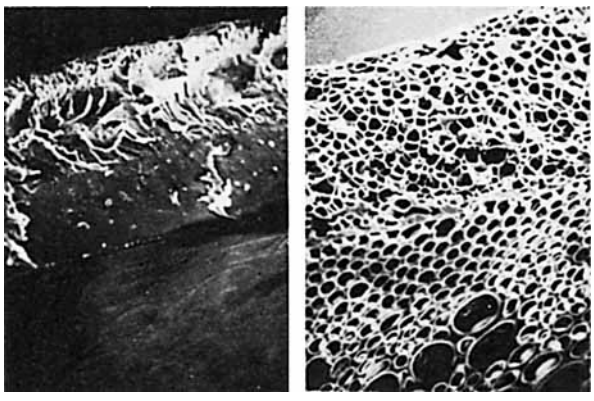

Fig. 4. Scanning electron micrographs for PVC homopolymer (100/0) (a) and 30/70 (PVC/EBBA) composite membrane (b) after extracting EBBA with ethanol at 333 K for 2 h.

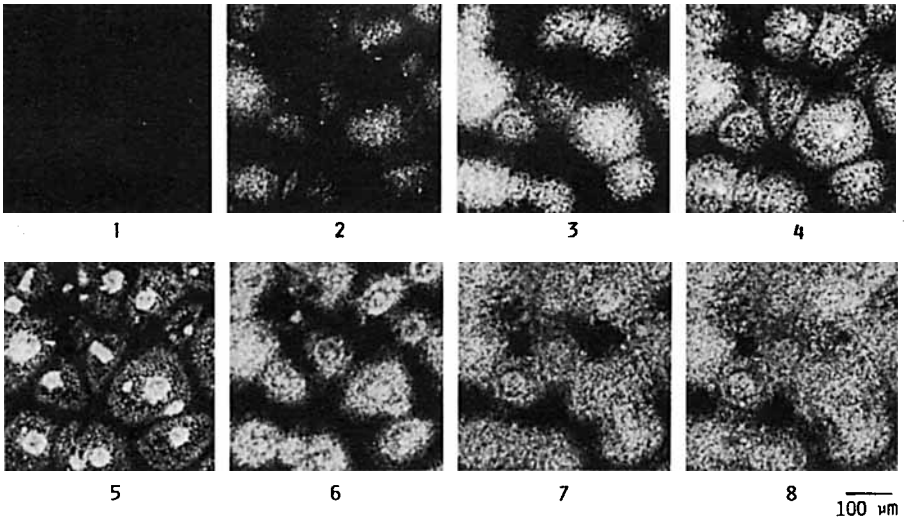

Fig. 5. Polarizing optical micrographs under crossed nicols during a solvent evaporation for 40/60 (PVC/EBBA) composite membrane at 293 K ($< T_{KN}$).

tographs for the 40/60 (PVC/EBBA) composite membrane at the temperature of 293 K ($< T_{KN}$) upon a solvent evaporation. In the case of an isotropic liquid state just after casting, a field of vision was dark [Fig. 5 (1)]. Liquid crystalline molecules were gradually clustering or aggregating with a solvent evaporation, resulting in an exclusion of PVC molecules a shown by a dark field in Figure 5 (2). At a certain concentration, the crystallite-like domains of EBBA were produced and began to grow in PVC matrix [Fig. 5 (3)–(8)]. Simultaneously, an excluded PVC phase surrounded EBBA crystal domains as the networks in a similar manner to a coacervation effect.[8,9] Consequently, distinct crystal domains of EBBA were formed in the composite membrane as a continuous phase and the characteristic interpenetrated structure composed of both components was completed in this process. Of course, the diameter of the EBBA cluster in Figure 5 is greater than that of holes in Figure 3. The EBBA clusters may be divided into smaller ones, though the surrounding PVC networks cannot be distinguished under POM.

Mechanical Properties

Figure 6 shows the stress-strain curves for a series of PVC/EBBA composite membranes at several weight fractions of EBBA (at 293 K, $< T_{KN}$). The initial modulus E, the stress at break σ_b, and the strain at break ϵ_b are summarized in Table I. The values of E for the PVC/EBBA composite membranes decreased with an increase in the weight fraction of EBBA, but ϵ_b increased to the contrary up to 45 wt % of EBBA in comparison with that for PVC homopolymer (100/0). Also, the values of E for composite membranes at above the EBBA fraction of 60 wt % increased again, which might be due to the contribution from the continuous crystal phase of EBBA. In particular, the 40/60 (PVC/EBBA) composite membrane, for which the gas permeation characteristics were investigated in this study, exhibited

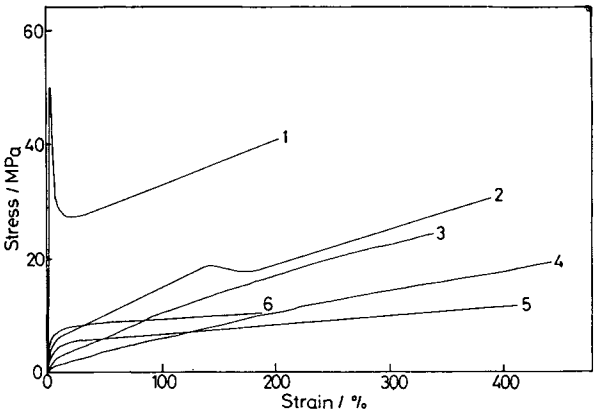

Fig. 6. Stress-strain curves for a series of PVC/EBBA composite membranes at several weight fractions of EBBA (at 293 K, $< T_{KN}$):(1) 100/0; (2) 85/15; (3) 70/30; (4) 55/45; (5) 40/60; (6) 30/70.

an excellent ductility, that is, $\epsilon_b = 413\%$. In contrast with this, a series of PC/EBBA composite membranes were fairly brittle,[10] that is, $\epsilon_b = 3.3.5\%$ for 40/60 (PC/EBBA) composite membrane. In the case of practical applications as a permselective membrane, the ductile properties of membrane are required from a veiwpoint of preparation of ultrathin films. Then, the mechanical property for the 40/60 (PVC/EBBA) composite membrane proved to suffice for such a requirement. As mentioned above, the composite membrane is composed of the interpenetrating continuous phases of liquid crystalline molecules and polymer matrix. This kind of aggregation state should provide the excellent mechanical properties or stabilities to composite membranes.

Permeation Characteristics to Oxygen and Nitrogen Gases

Figure 7 shows the Arrhenius plots of the permeability coefficients P to oxygen and nitrogen gases for the 40/60 (PVC/EBBA) composite membrane. The oxygen permeability coefficient P_{O_2} and the nitrogen one P_{N_2} are summarized in Table II, together with the corresponding separation factor, P_{O_2}/P_{N_2} as a function of measuring temperatures. From Figure 7 and Table II, it is apparent that the values of P_{O_2} are of the order of 10^{-11}--^{10}cm^3 (STP) cm^{-1} s^{-1} cm Hg^{-1} in a temperature range below T_{KN}, while of the order of

TABLE I
Mechanical Properties for A Series of PVC/EBBA Composite Membranes at Several Weight Fractions of EBBA (at 293 K, $< T_{KN}$)

Sample PVC/EBBA (wt %)	E (GPa)	σ_b (MPa)	ϵ_b (%)
100/0	2.54	41.1	205
85/15	0.235	30.1	390
70/30	0.0480	24.0	339
55/45	0.0142	18.8	444
40/60	0.144	11.7	413
30/70	0.236	10.0	189

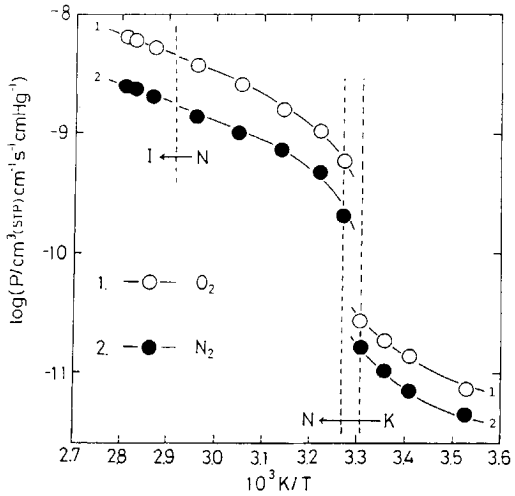

Fig. 7. Arrhenius plots of permeability coefficient P to oxygen and nitrogen gases for 40/60 (PVC/EBBA) composite membrane: (1) O_2; (2) N_2.

10^{-9} cm³(STP) cm^{-1} s^{-1} cm Hg^{-1} above T_{KN}. As mentioned above, a liquid crystalline phase takes a role of a main mobile region for permeant gas molecules, because the magnitude of viscosity in a nematic liquid crystalline state of EBBA is of the same order as that of water.[11] In other words, the temperature dependence of P for the polymer/liquid crystal composite membrane is closely related not only to the thermal molecular motion of components but to the domain size or continuity of liquid crystalline phase. In consideration of the aggregation state of the composite membrane, it seems reasonable that the magnitude of P discontinuously increased by about 20–30 times within a few degree of temperature in the vicinity of the crystal-liquid crystal transition region as shown in Figure 7.

Figure 8 shows the plots of the separation factor P_{O_2}/P_{N_2} against P_{O_2} for the 40/60 (PVC/EBBA) composite membrane (curve 1 in Fig. 8), compared

TABLE II
Oxygen Permeability Coefficient P_{O_2}, Nitrogen One P_{N_2}, and separation factor P_{O_2}/P_{N_2} for 40/60 (PVC/EBBA) Composite Membrane as a Function of Temperature

PVC/EBBA = 40/60	Temp (K)	$P_{O_2} \times 10^{10}$ (cm³(STP) · cm^{-1} · s^{-1} · cm Hg^{-1})	$P_{N_2} \times 10^{10}$ (cm³(STP) · cm^{-1} · s^{-1} · cm Hg^{-1})	P_{O_2}/P_{N_2}
Crystal	283	0. 0794	0.0457	1.74
	293	1.135	0.0708	1.91
	298	0.182	0.100	1.82
	302	0.268	0.151	1.77
Nematic	307	5.75	1.95	2.95
	311	10.6	4.27	2.48
	318	17.0	7.24	2.34
	328	24.6	9.96	2.47
	338	37.4	13.6	2.75
Isotropic	348	51.9	20.6	2.52
	353	60.6	24.1	2.51
	356	63.7	24.7	2.54

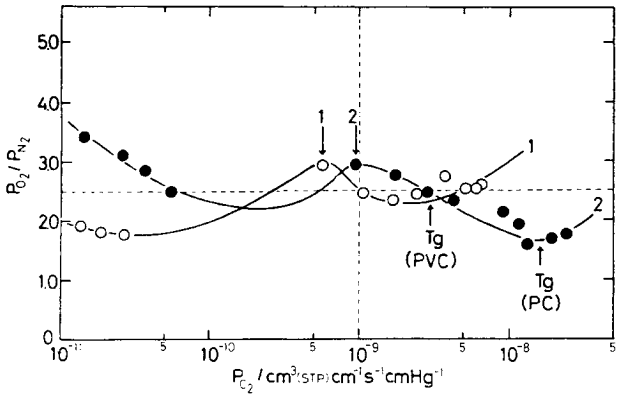

Fig. 8. A plot of separation factor P_{O_2}/P_{N_2} against oxygen permeability coefficient, P_{O_2} for (1) 40/60 (PVC/EBBA) and (2) 40/60 (PC/EBBA) composite membranes.

with those for the PC/EBBA one (curve 2). An increase in P_{O_2} on the abscissa corresponds to a rise of measuring temperature. The broken lines describes the conventional lower limits for practical applications as an oxygen enrichment membrane, that is, $P_{O_2} = 10^{-9}$ cm³(STP) · cm^{-1} · s^{-1} · cm Hg^{-1} and $P_{O_2}/P_{N_2} = 2.5$. For both composite membranes, the magnitudes of P_{O_2} and P_{N_2} were approximately of the same order at the corresponding temperatures with respect to T_{KN}, and, also, the separation factor of oxygen to nitrogen gases showed a maximum excursion around the phase transition region (T_{KN}) as exhibited by an arrow in Figure 8. As mentioned in our previous papers,[4,7] the gas permeation characteristics through the polymer/liquid crystal composite membrane change from the diffusion-controlled permeation to the solubility-controlled one beyond T_{KN}. Furthermore, the magnitude of the solubility coefficient takes a maximum value at around T_{KN} and a composite membrane with the surface covered by EBBA molecules have a stronger affinity for oxygen gas than nitrogen one. Therefore, on the assumption that the diffusion coefficients to oxygen and nitrogen gases are of the same order, it seems reasonable that the solubility characteristics gave the maximum separation factor at around T_{KN}.

Next, we will discuss an unusual permeation behavior with respect to the $P_{O_2}-P_{O_2}/P_{N_2}$ relationship. In general, the magnitude of separation factor decreases with an increase in the permeability coefficient. However, the opposite tendency was observed for the PVC/EBBA and PC/EBBA composite membranes, i.e., P_{O_2}/P_{N_2} increased with an increase in P_{O_2} in a higher temperature range above the glass transition temperatures of respective matrix polymers. Though the reasons for this unique relationship on $P_{O_2}-P_{O_2}/P_{N_2}$ has not been directly clarified yet, it seems undoubted that this behavior is closely related to the contribution from the glass transition of matrix polymer. There is a good assumption to elucidate this unique trend: A gas sorption surface composed of liquid crystalline material may be freshly supplied by the activated thermal molecular motion of matrix polymer at around T_g, and, also, the excellent oxygen selectivity of matrix polymer[12] may begin to contribute a further increase in permselectivity above T_g. Then, the PVC/EBBA composite membrane has a possibility as a characteristic permselective membrane for oxygen.

CONCLUSIONS

EBBA in PVC/EBBA composite membranes is molecularly dispersed at below the EBBA fraction of 30 wt %, and, also, it exists in both states of molecular dispersion and crystal domains in the case of the EBBA fraction at above 45 wt %. EBBA in the 40/60 and 30/70 (PVC/EBBA) composite membranes forms a continuous phase in the 3-dimensional spongy networks of PVC matrix. The PVC/EBBA composite membrane has a high mechanical durability or flexibility compared with the PC/EBBA composite membrane. This mechanical property is advantageous to prepare an ultrathin composite membrane. The permeability coefficients to oxygen and nitrogen gases increase with an apparent jump by 20–30 times within a few degrees in the vicinity of the crystal–nematic transition temperature of EBBA. The relationship between the oxygen permeability and its selectivity exhibites a unique tendency as P_{O_2}/P_{N_2} increases with an increase in P_{O_2}.

References

1. R. M. Barrer, *Diffusion in Polymers* J. Crank and G. S. Park, Eds., Academic, London and New York, 1968, Chap. 4.
2. W. J. Ward, W. R. Browall, and R. M. Salamme, *J. Membr. Sci,*. **1**, 99 (1976).
3. D. L. MacLean and T. E. Graham, *Chem. Eng. News,* **19**, 57 (1980).
4. T. Kajiyama, Y. Nagata, S. Washizu, and M. Takayanagi, *J. Membr. Sci.*, **11**, 39 (1982).
5. S. Washizu, T. Kajiyama, and M. Takayanagi, *J. Chem. Soc. Jpn.*, **1983**, 838.
6. R. M. Barrer and G. Skirrow, *J. Polym. Sci.*, **3**, 549 (1948).
7. S. Washizu, I. Terada, T. Kajiyama, and M. Takayanagi, *Polym. J.*, **16**, (1984) to appear.
8. R. E. Kesting, *J. Macromol. Sci.-Chem., A4,* **3**, 665 (1970).
9. K. Maier and E. Scheuermann, *Kolloid Z.*, **171**, 122 (1960).
10. S. Washizu, I. Terada, T. Kajiyama, and M. Takayanagi, *Polym. Prepr, Jpn.*, **32**, 2973 (1983).
11. R. S. Porter and J. F. Johnson, *J. Appl. Phys.*, **34**, 51 (1963).
12. T. Nakagawa, H. B. Hopfenberg, and V. T. Stannett, *J. Appl. Polym. Sci.*, **15**, 231 (1971).

Received February 10, 1984
Accepted April 4, 1984